



AKADÉMIAI KIADÓ

Pollack Periodica •
An International Journal
for Engineering and
Information Sciences


17 (2022) 2, 98–103

DOI:
[10.1556/606.2021.00482](https://doi.org/10.1556/606.2021.00482)
© 2021 Akadémiai Kiadó, Budapest

ORIGINAL RESEARCH
PAPER



Study of the strengthened state near the forces for the semi-plan

Drakuli Lumi^{1*} , Anis Sulejmani¹, Klodian Dhoska² and Odhise Koça¹

¹ Department of Mechanics, Faculty of Mechanical Engineering, Polytechnic University of Tirana, Mother Theresa Square, No. 4, Tirana, Albania

² Department of Production and Management, Faculty of Mechanical Engineering, Polytechnic University of Tirana, Mother Theresa Square, No. 4, Tirana, Albania

Received: August 5, 2021 • Revised manuscript received: November 4, 2021 • Accepted: November 5, 2021
Published online: December 15, 2021

ABSTRACT

Many of the engineering applications have faced the delicate contact problem in the area close to the forces where it is very difficult to experimentally carry out various measurements and draw important conclusions on the condition of the contact points. In this paper the forced state in the vicinity of the forces for the half-plane will be studied. Furthermore, the qualities displayed by the half-plane under the action of normal forces, tangential forces and the moment caused by a pair of forces will be analyzed, as well as changes in the elastic characteristics for the forced plane state and the deformed plane state.

KEYWORDS

forced state, geometric points, elastic characteristics, biharmonic function

1. INTRODUCTION

Many interests of the engineering researchers have been focused in the delicate contact problem in the area close to the forces for different engineering applications [1–10]. Contact mechanics has its application in many engineering problems. Some examples of the small deformation contact problems come from interaction between soil and foundations in civil engineering or general bearing problems as well as bolt and screw joints in mechanical engineering [1, 5, 10]. From the other side an example for large deformation contact has been come from the impact of cars through car tire-road interaction and metal forming [10].

These important examples that have been mentioned above in relation to the deformation contact problems have increased interest to focused in current research work at the most delicate problem in the area close to the forces due to the difficulties for carrying out various measurements and draw important conclusions on the condition of the contact points. The aim of this paper is to study the forced state in the vicinity of the forces for the half-plane. Furthermore, the qualities displayed by the half-plane under the action of normal forces, tangential forces and the moment caused by a pair of forces should be analyzed as well as the changes in the elastic characteristics for the forced plane state and the deformed plane state.

2. SYMMETRICAL AND ANTI-METRIC LOADING WITH NORMAL CONTACT PRESSURE

The representation of the symmetric and anti-metric load is given in Fig. 1.

For external anti-metric loading, broken down into trigonometric series of form [1]:

*Corresponding author.
E-mail: lumidrakuli@gmail.com

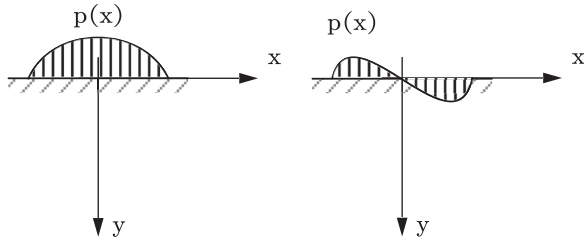


Fig. 1. Distributed symmetrical and anti-metric load

$$p(x) = \sum_{n=1}^{\infty} p_n \cdot \sin \alpha_n x. \quad (1)$$

It has been chosen the harmonic function of the form:

$$\Phi(x, y) = \sum_{n=1}^{\infty} R(y) \cdot e^{-\alpha_n y} \cdot \sin \alpha_n x, \quad (2)$$

$$\Phi(x, y) = \left(\frac{C_1}{2 \cdot \alpha} - \frac{C_2}{4 \cdot \alpha^2} \cdot \frac{e^{2\alpha y}}{2 \cdot \alpha} + \frac{C_2}{4 \cdot \alpha^2} \cdot e^{2\alpha y} \cdot \left(y - \frac{1}{2 \cdot \alpha} \right) + C_3 \cdot y + C_4 \right) \cdot e^{-\alpha y} \cdot \sin \alpha x. \quad (3)$$

From the static conditions in the contour ($y = 0$), we obtain the relations:

$$\sigma_{yy} = -\alpha_n^2 \cdot \sin \alpha_n x \cdot \left(C_4 + \frac{C_1}{4 \cdot \alpha_n^2} - \frac{C_2}{4 \cdot \alpha_n^3} \right) = p_n \cdot \sin \alpha_n x, \quad (4)$$

$$\sigma_{xy} = -\alpha_n \cdot \cos \alpha_n x \cdot (-\alpha_n \cdot R(y) + R'(y)) \cdot e^{-\alpha_n y} = 0. \quad (5)$$

Accepting $C_1 = C_2 = 0$, take $C_3 = -p_n/\alpha$ and $C_4 = -p_n/\alpha^2$.

Finally, the harmonic function comes out of shape:

$$\Phi_n(x, y) = (\alpha \cdot y - 1) \cdot \frac{e^{-\alpha_n y} \cdot \sin \alpha_n x}{\alpha^2} \cdot p_n. \quad (6)$$

In contrast, for the symmetric load [11], it will have the expressions:

$$p(x) = p_0 + \sum_{n=1}^{\infty} p_n \cdot \cos \alpha_n x. \quad (7)$$

$$\Phi_n(x, y) = -(1 + \alpha \cdot y) \cdot \frac{e^{-\alpha_n y} \cdot \cos \alpha_n x}{\alpha^2} \cdot p_n. \quad (8)$$

3. FOURIER INTEGRALS IN LOCAL LOAD DECOMPOSITION

In the contour area $0 \leq \theta \leq 2\pi$, the function $p(\theta)$ decomposes into Fourier series to form:

$$p(\theta) = p_0 + \sum_{n=1}^{\infty} p_n \cdot \cos n\theta + t_n \cdot \sin n\theta. \quad (9)$$

$$p_n = -\frac{1}{\pi} \int p(\theta) \cos n\theta d\theta, \quad t_n = -\frac{1}{\pi} \int p(\theta) \sin n\theta d\theta. \quad (10)$$

Substituting according to Euler: $e^{in\theta} = \cos n\theta + i \cdot \sin n\theta$, $\cos n\theta = (e^{in\theta} + e^{-in\theta})/2$, $i \cdot \sin n\theta = (e^{in\theta} - e^{-in\theta})/2$. It will get the other presentation form of equation (9):

$$p(\theta) = p_0 + \sum_{n=1}^{\infty} p_n \cdot e^{in\theta} + t_n \cdot e^{-in\theta}. \quad (11)$$

Knowing that $\int_0^{2\pi} e^{in\theta} d\theta = \begin{cases} 0, & \text{for } n \text{ integers,} \\ 2\pi, & \text{for } n = 0, \end{cases}$ takes:

$$p_n = \frac{1}{2\pi} \int_0^{2\pi} p(\theta) e^{in\theta} d\theta. \quad (12)$$

The local charge is presented in the form:

$$p(x) = \sum_{-\infty}^{\infty} p_n \cdot e^{i\alpha_n x}, \quad p_n = \frac{1}{2\pi} \int_0^{2\pi} p(\xi) e^{i\alpha_n \xi} d\xi, \quad (13)$$

and

$$p(x) = \frac{1}{2\pi} \int_{-\infty}^{\infty} \int_{-\infty}^{\infty} p(\xi) e^{i\alpha(\xi-x)} d\alpha d\xi. \quad (14)$$

For the symmetric local charge and for the anti-metric charge, would have reciprocal expressions in Eqs (14) and (15):

$$b(\alpha) = \frac{2}{\pi} \int_0^{\infty} p(\xi) \cos \alpha \xi d\xi, \quad p(x) = \int_0^{\infty} b(\alpha) \cos \alpha x d\alpha, \quad (15)$$

$$a(\alpha) = \frac{2}{\pi} \int_0^{\infty} p(\xi) \sin \alpha \xi d\xi, \quad p(x) = \int_0^{\infty} a(\alpha) \sin \alpha x d\alpha. \quad (16)$$

4. THE FORCED STATE FOR THE HALF-PLANE WITH NORMAL FORCE

Concentrated force is seen in Fig. 2 as the limit of a uniformly distributed load over an infinitesimally small area $2 \cdot \varepsilon$. Then the load turns out to be a normal symmetric local [1, 11], so it has the ready solution (16).

After performing the actions, have:

$$\begin{aligned} b(\alpha) &= \lim_{\varepsilon \rightarrow 0} \frac{2}{\pi} \int_0^{\infty} p(\xi) \cos \alpha \xi d\xi = \frac{2}{\pi} \lim_{\varepsilon \rightarrow 0} \int_0^{\infty} \frac{F}{2\varepsilon} \cos \alpha \xi d\xi = \\ &= \frac{2}{\pi} \lim_{\varepsilon \rightarrow 0} \frac{P}{2\varepsilon} \frac{\sin \alpha \varepsilon}{\alpha} = \frac{F}{\pi}, \end{aligned} \quad (17)$$

$$p(x) = \frac{P}{\pi} \int_0^{\infty} \cos \alpha x d\alpha. \quad (18)$$

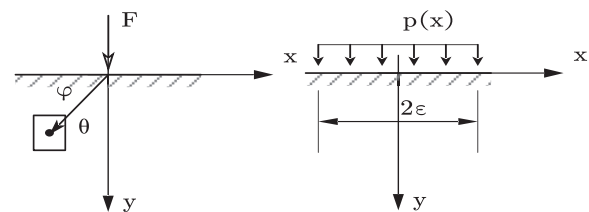
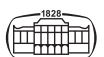


Fig. 2. Compressive force in the infinite half-plane



For normal symmetric loading the biharmonic function takes the form:

$$\Phi(x, y) = -\frac{F}{\pi} \int (1 + \alpha \cdot y) \cdot \frac{e^{-\alpha \cdot y} \cdot \cos \alpha x}{\alpha^2} \cdot d\alpha = \frac{F}{\pi} x \cdot \arctg \frac{y}{x}. \quad (19)$$

The strains are given by the expressions:

$$\sigma_{xx} = \frac{\partial^2 \Phi}{\partial y^2} = \frac{F}{\pi} \int (1 - \alpha \cdot y) \cdot \frac{e^{-\alpha \cdot y} \cdot \cos \alpha x}{1} \cdot d\alpha = -\frac{2F}{\pi} \frac{x^2 y}{(x^2 + y^2)^2}, \quad (20)$$

$$\sigma_{yy} = \frac{\partial^2 \Phi}{\partial x^2} = \frac{F}{\pi} \int (1 + \alpha \cdot y) \cdot \frac{e^{-\alpha \cdot y} \cdot \cos \alpha x}{1} \cdot d\alpha = -\frac{2F}{\pi} \frac{y^3}{(x^2 + y^2)^2}, \quad (21)$$

$$\sigma_{xy} = -\frac{\partial^2 \Phi}{\partial x \partial y} = \frac{F}{\pi} \int (y) \cdot \frac{e^{-\alpha \cdot y} \cdot \sin \alpha x}{1} \cdot d\alpha = -\frac{2F}{\pi} \frac{xy^2}{(x^2 + y^2)^2}. \quad (22)$$

Element taken in the vertical plane $x = x_0$, detects strains σ_{xx} , σ_{yx} with their extreme values as it can be seen in Fig. 3: $\sigma_{xx}^{\max} = 3\sqrt{3}F/8\pi x_0$, in $y = \frac{x_0}{\sqrt{3}}$, $\sigma_{yx}^{\max} = F/2\pi x_0$, in $y = x_0$.

Extreme values of σ_{xx}^{\max} are according to the line emanating from the origin at an angle $\tan \theta = \sqrt{3} \gg \theta = 60^\circ$, whereas the extreme values of σ_{yx}^{\max} are according to the line emanating from the origin at an angle $\tan \theta = 1 \gg \theta = 45^\circ$.

Element taken in the horizontal plane $y = y_0$, detects strains σ_{yy} , σ_{xy} with their extreme values are shown in Fig. 4:

$$\sigma_{yy}^{\max} = \frac{2F}{\pi y_0}, \text{ in } x = 0, \quad \sigma_{xy}^{\max} = \frac{3\sqrt{3}F}{8\pi y_0}, \text{ in } x = \frac{y_0}{\sqrt{3}}. \quad (23)$$

The displacements, when the strain function is known, will be:

$$E \cdot u = -\frac{P}{\pi} \int \frac{1}{\alpha} [1 - \mu + \alpha y(1 + \mu)] e^{-\alpha y} \sin \alpha x \, d\alpha, \quad (24)$$

$$E \cdot (v - c) = -\frac{P}{\pi} \int \frac{1}{\alpha} [2 + \alpha y(1 + \mu)] e^{-\alpha y} \cos \alpha x \, d\alpha, \quad (25)$$

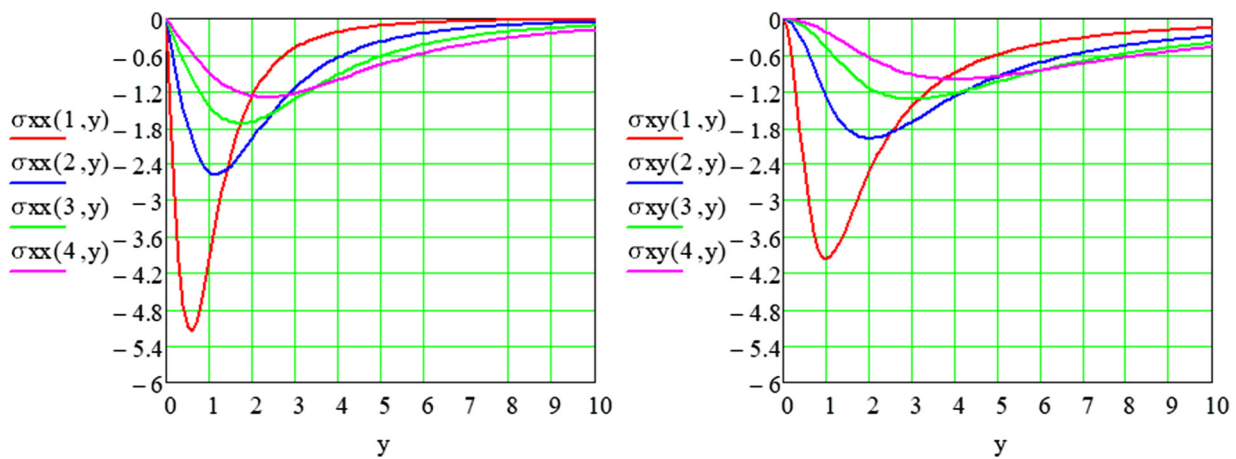


Fig. 3. Strains in the vertical planes σ_{xx} , σ_{xy} in N mm^{-2} , x in mm, results are obtained for $F = 100 \text{ N}$

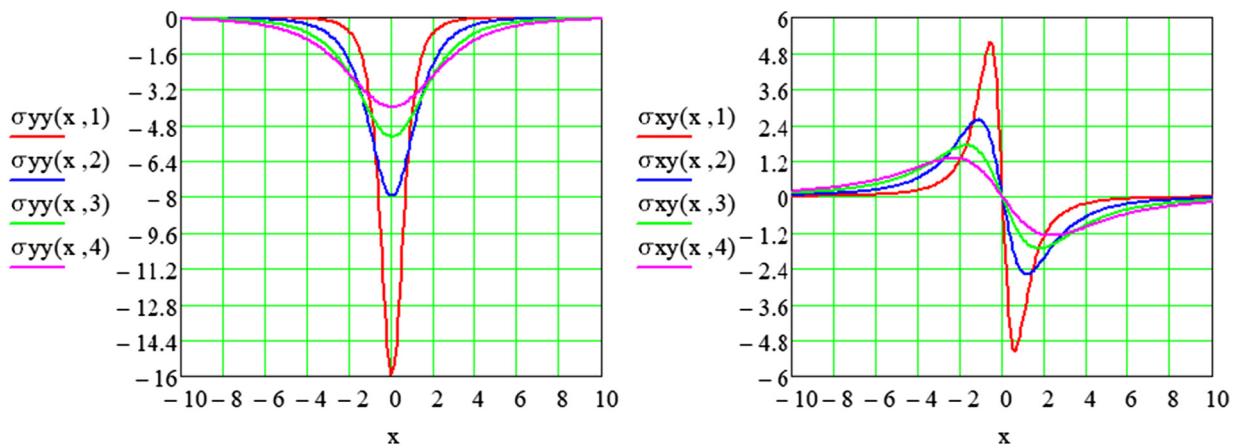


Fig. 4. Strains in the horizontal planes σ_{yy} , σ_{xy} in N mm^{-1} , x in mm, results are obtained for $F = 100 \text{ N}$

where E in N mm^{-2} is Young Module and u , v and c are displacement in horizontal plane in mm.

In Fig. 5, after integration with the conditions $F = 100 \text{ N}$, $x = 0 \text{ mm}$, $y = 100 \text{ mm}$, $v = 0 \text{ mm}$, it has:

$$E \cdot u = -\frac{100}{\pi} \left[(1 - \mu) \cdot \arctg \frac{x}{y} - (1 + \mu) \cdot \frac{xy}{x^2 + y^2} \right], \quad (26)$$

$$E \cdot v = -\frac{100}{\pi} \left[\ln(x^2 + y^2) - (1 + \mu) \cdot \frac{y^2}{x^2 + y^2} \right] + 252.43 \text{ N mm}^{-1}. \quad (27)$$

5. THE FORCED STATE FOR THE HALF-PLANE WITH TANGENTIAL FORCE

Figure 6 depicts the tangential forces on the half-plane:

Concentrated force is seen as the limit of a uniformly distributed load over an infinitesimally small area $2 \cdot \varepsilon$.

The strains were:

$$\begin{aligned} \sigma_{xx} &= \frac{\partial^2 \Phi}{\partial y^2} = -\frac{2P}{\pi} \frac{x^3}{(x^2 + y^2)^2}, \\ \sigma_{yy} &= \frac{\partial^2 \Phi}{\partial x^2} = -\frac{2P}{\pi} \frac{y^3}{(x^2 + y^2)^2}, \\ \sigma_{xy} &= \frac{\partial^2 \Phi}{\partial x \partial y} = -\frac{2P}{\pi} \frac{x^2 y}{(x^2 + y^2)^2}. \end{aligned} \quad (28)$$

Figure 7 shows the horizontal strains.

Element taken in the vertical plane $x = x_0$ detects strains σ_{xx} , σ_{yx} with their extreme values of:

$$\sigma_{xx}^{\max} = \frac{2F}{\pi x_0}, \quad \text{in } y = 0, \quad \sigma_{yx}^{\max} = \frac{9 \cdot F}{8 \cdot \pi \cdot \sqrt{3} \cdot x_0}, \quad \text{at } y = \frac{x_0}{\sqrt{3}}. \quad (29)$$

Extreme values of σ_{xx}^{\max} are according to the line emanating from the origin at an angle $\tan \theta = 0 \gg \theta = 0^\circ$, whereas the extreme values of σ_{yx}^{\max} are according to the line emanating

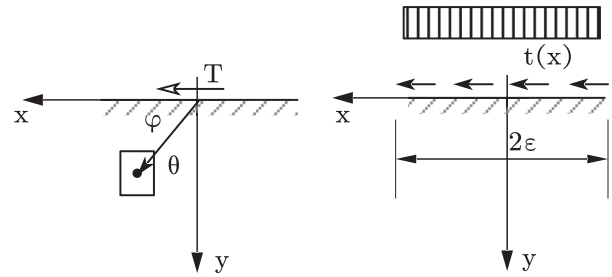


Fig. 6. Tangential force in the infinite half-plane

from the origin at an angle $\tan \theta = \sqrt{3} \gg \theta = 60^\circ$. Elements that have taken in the horizontal plane $y = y_0$ detects strains σ_{yy} , σ_{xy} with their extreme values:

$$\sigma_{yy}^{\max} = \frac{9 \cdot F}{8 \cdot \pi \cdot \sqrt{3} \cdot y_0}, \quad \text{in } x = \frac{y_0}{\sqrt{3}}; \quad \sigma_{xy}^{\max} = \frac{F}{2\pi y_0}, \quad \text{at } x = y_0. \quad (30)$$

Extreme values of σ_{yy}^{\max} are according to the line emanating from the origin at an angle $\tan \theta = 1 \gg \theta = 45^\circ$, whereas the extreme values of σ_{xy}^{\max} are according to the line emanating from the origin at an angle $\tan \theta = \frac{1}{\sqrt{3}} \gg \theta = 30^\circ$.

The displacements will be:

$$E \cdot u = -\frac{F}{\pi} \left[\ln(x^2 + y^2) - (1 + \mu) \cdot \frac{y^2}{x^2 + y^2} \right] - E \cdot (\omega_0 y - u_0), \quad (31)$$

$$E \cdot v = -\frac{F}{\pi} \left[(1 - \mu) \cdot \arctg \frac{x}{y} - (1 + \mu) \cdot \frac{xy}{x^2 + y^2} \right] + E \cdot \omega_0 x. \quad (32)$$

Displacement of points on the surface $x = x$ and $y = 0$, will be:

$$E \cdot (u - u_0) = -\frac{2 \cdot F}{\pi} \cdot \ln(|x|); \quad E \cdot (v - \omega_0 x) = \frac{P}{2} \cdot (1 - \mu). \quad (33)$$

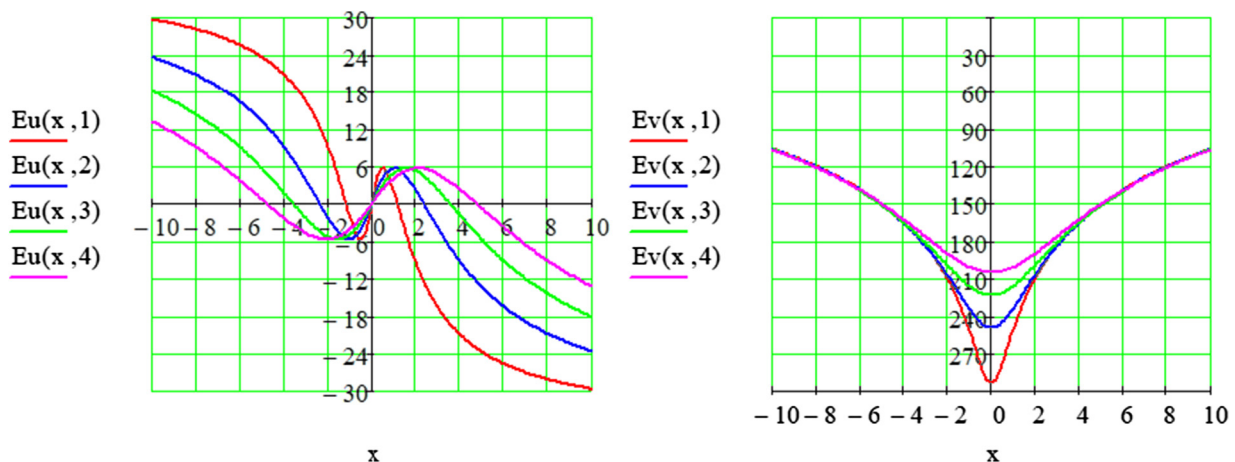


Fig. 5. Displacement u and v in the horizontal planes, results are obtained for $F = 100 \text{ N}$, $\mu = 0.28$, x in mm

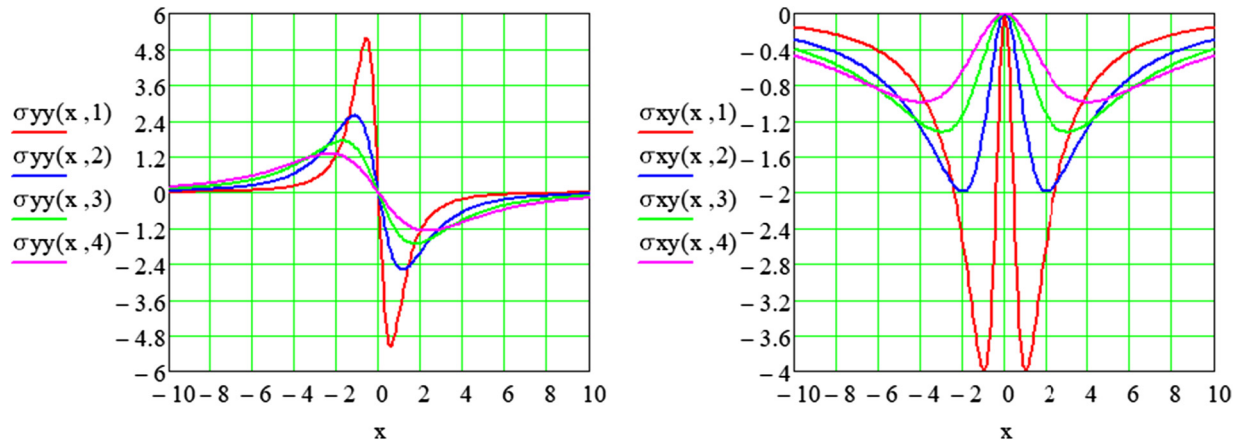


Fig. 7. Strains in the horizontal planes σ_{yy} , σ_{xy} in N mm^{-1} , x in mm

With the conditions $F = 100 \text{ N}$, $x = 0 \text{ mm}$, $y = 100 \text{ mm}$, $u = 0 \text{ mm}$ and $x = 100 \text{ mm}$, $y = 100 \text{ mm}$, $v = 0 \text{ mm}$, have: $E \cdot \omega_0 = -0.0237 \text{ N mm}^{-1}$ and $E \cdot u_0 = 250.05 \text{ N mm}^{-1}$.

From the analysis of point displacements, it is noticed that the horizontal displacements are all in one direction, while the vertical displacements close to the force, in front of it rise.

6. THE FORCED STATE FOR THE HALF-PLANE WITH FORCE PAIR

Figure 8 depicts the couple of forces on the half-plane:

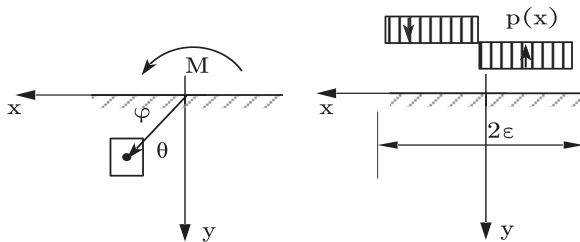


Fig. 8. Couple of forces in the half-plane

It has been seen the pair of forces as the limit of two forces, which in turn we see as the limit of a uniformly distributed load:

$$p = \frac{P}{\varepsilon} = \frac{M}{\varepsilon^2}. \quad (34)$$

Figure 9 shows the strains in the horizontal plan.

The strains are given by the expressions:

$$\sigma_{xx} = \frac{\partial^2 \Phi}{\partial y^2} = -\frac{4M}{\pi} \frac{xy(x^2 - y^2)}{(x^2 + y^2)^3}, \quad (35)$$

$$\sigma_{yy} = \frac{\partial^2 \Phi}{\partial x^2} = -\frac{8M}{\pi} \frac{xy^3}{(x^2 + y^2)^3}, \quad (36)$$

$$\sigma_{xy} = \frac{\partial^2 \Phi}{\partial x \partial y} = -\frac{2M}{\pi} \frac{y^2(3x^2 - y^2)}{(x^2 + y^2)^3}. \quad (37)$$

The displacement will be:

$$E \cdot u = \frac{2M}{\pi} \cdot \frac{y \cdot (x^2 - y^2)}{(x^2 + y^2)^2} - E \cdot \omega_0 \cdot y, \quad (38)$$

$$E \cdot v = \frac{2M}{\pi} \cdot \frac{x \cdot (x^2 + y^2 \cdot (2 + \mu))}{(x^2 + y^2)^2} + E \cdot \omega_0 \cdot x. \quad (39)$$

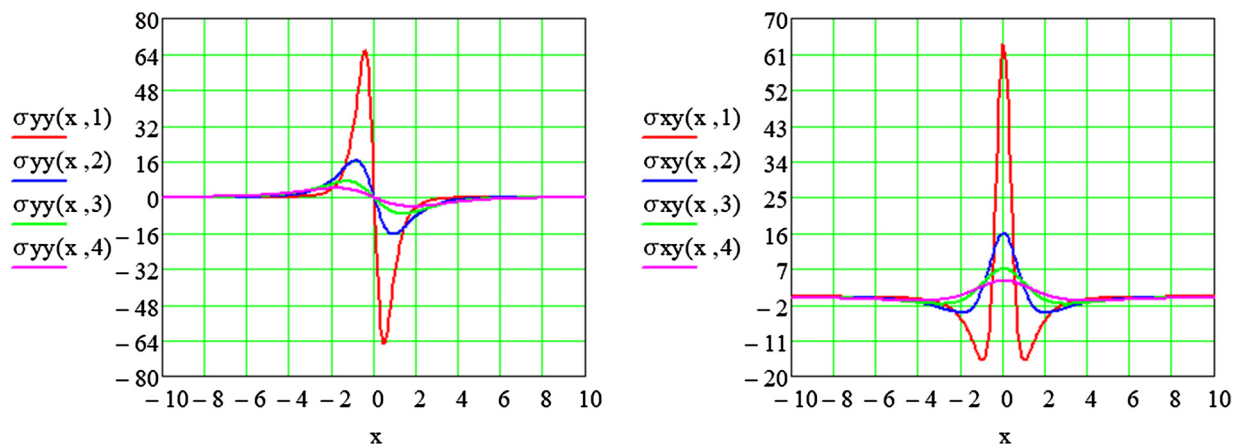


Fig. 9. Strains in the horizontal planes σ_{yy} , σ_{xy} , with the conditions $M = 100 \text{ Nm}$ and x in mm

7. CONCLUSIONS

Based on analytical research study following conclusions were drawn:

- The plan problem in strains comes down to defining only one accordion function $\Phi(x, y)$, which satisfies the static and kinematic conditions in the contour of elastic bodies;
- The geometric location of the points in semi-plane with normal force and tangential force half-plane where the maximum strains take extreme values for horizontal and vertical planes represent straight lines emanating from the origin σ_{xx} , σ_{yx} , σ_{xy} , σ_{yy} ;
- In tangential force half-plane, it has been seen that the vertical axis Oy consists of points with zero principal strain where this line separates the half plane in the traction part from the compression part;
- Isochrones at tangential force half-plane were circles centered on the Ox axis and tangent to the Oy axis but at semi-plane in normal force were circles centered on the Oy axis and tangent to the Ox axis.

REFERENCES

- [1] O. Koça, A. Sulejmani, and K. Dhoska, "Pressure distribution on rolling-slide contact problem," *Pollack Period.*, vol. 16, no. 1, pp. 71–76, 2021.
- [2] O. Koça, A. Sulejmani, and K. Dhoska, "The strenuous state of the contact at the sliding-flip pairs," *Machines, Technol. Mater.*, vol. 14, no. 7, pp. 258–261, 2020.
- [3] O. Koça and F. G. Buchholz, "A stress analysis for contact problems involving rolling and sliding," *WIT Trans. Eng. Sci.*, vol. 1, pp. 127–134, 1993.
- [4] A. Vinko, "Monitoring and condition assessment of tramway track using in-service vehicle," *Pollack Period.*, vol. 11, no. 3, pp. 73–82, 2016.
- [5] S. B. Wani, "Analytical study on the influence of rib beams on the stability of RCC dome structures," *Int. J. Innovative Technol. Interdiscip. Sci.*, vol. 3, no. 3, pp. 480–489, 2020.
- [6] A. Pramono, K. Dhoska, I. Markja, and L. Kommel, "Impact pressure on mechanical properties of aluminum based composite by ECAP-parallel channel," *Pollack Period.*, vol. 14, no. 1, pp. 67–74, 2019.
- [7] R. Nagy, "Description of rail track geometry deterioration process in Hungarian rail lines No. 1 and No. 140," *Pollack Period.*, vol. 12, no. 3, pp. 141–156, 2017.
- [8] K. Dhoska, S. Tola, A. Pramono, and I. Vozga, "Evaluation of measurement uncertainty for the determination of the mechanical resistance of the brick samples by using uniaxial compressive strength test," *Int. J. Metrology Qual. Eng.*, vol. 9, no. 12, pp. 1–5, 2018.
- [9] S. A. Hasani, Nasrellah A. H, and A. A. Abdulraeg "Numerical study of reinforced Concrete beam by using ABAQUS software," *Int. J. Innovative Technol. Interdiscip. Sci.*, vol. 4, no. 3, pp. 733–741, 2021.
- [10] S. Vulovic, M. Zivkovic, N. Grujovic, and R. Slavkovic, "A comparative study of contact problems solution based on the penalty and Lagrange multiplier approaches," *J. Serbian Soc. Comput. Mech.*, vol. 1, no. 1, pp. 174–183, 2007.
- [11] O. Koca and F. G. Buchholz, "Analytical and computational stress analysis of fiber/matrix composite models," *Comput. Mater. Sci.*, vol. 3, no. 9, pp. 135–145, 1994.